Fitoterapia 134 (2019) 411–416

Contents lists available at ScienceDirect

Fitoterapia

journal homepage: www.elsevier.com/locate/fitote

Zizhines G–O, AchE inhibitory meroterpenoids from *Ganoderma sinensis*

Qi Luo[a,1], Wen-Wen Cao[a,c,1], Ze-Hong Wu[b,1], Shu-Mei Wang[c], Yong-Xian Cheng[b,*]

[a] State Key Laboratory of Phytochemistry and Plant Resources in West China, Kunming Institute of Botany, Chinese Academy of Sciences, Kunming 650201, PR China
[b] Guangdong Key Laboratory for Genome Stability & Disease Prevention, School of Pharmaceutical Sciences, Shenzhen University Health Science Center, Shenzhen 518060, PR China
[c] Guangdong Pharmaceutical University, Guangzhou 510006, PR China

ARTICLE INFO

Keywords:
Ganoderma sinensis
Meroterpenoid
Zizhines G–O
AchE

ABSTRACT

Zizhines G–O (**1–9**), nine new meroterpenoids, and seven known analogs (**10–16**) were isolated from the dried fruiting bodies of *Ganoderma sinensis*. Their structures were identified by using spectroscopic data and CD curve comparison. The inhibitory activities of the selected new meroterpenoids toward AchE were assessed in vitro. Compounds **1–6** and **10–14** were found to exhibit AchE inhibitory activities at the concentration of 50 μM.

1. Introduction

Ganoderma, a group of wood degrading mushrooms with hard fruiting bodies, is a basidiomycete belonging to the Ganodermataceae, and has been used as a dietary supplement for health improvement in China for thousands of years [1]. The *Ganoderma* species are also used as remedies for the treatment of several ailments including hepatopathy, nephritis, hypertension, hyperlipemia, arthritis, neurasthenia, insomnia, bronchitis, asthma, gastric ulcers, arteriosclerosis, and so on [2]. Chemical constituents responsible for these indications are triterpenoids, polysaccharides, alkaloids, fatty acids, nucleotides, proteins, peptides, trace elements, and sterols etc. [3]. *G. sinensis*, mainly distributed in the eastern and southern regions of China, is one of only two embodied *Ganoderma* species collected by Pharmacopoeia of P.R. China (2015 edition). Previous chemical investigation on this species mainly focused on polysaccharides [4], lipids [5], and triterpenoids [6], meroterpenoids in this species were largely unexplored [3,7].

Our research group initiated the investigations on *Ganoderma* and characterized structurally diverse meroterpenoids from *Ganoderma* species [8,9]. As our continuing search for bioactive meroterpenoids from *Ganoderma* species, the title fungus was investigated, which resulted in the isolation of nine new meroterpenoids, zizhines G–O (**1–9**) and seven known analogs (**10–16**) (Fig. 1). Herein, we report the isolation, structural elucidation of these substances and their AchE inhibitory activities.

2. Results and discussion

Zizhine G (**1**), a yellowish gum, has the molecular formula $C_{30}H_{32}O_7$ with fifteen degrees of unsaturation deduced from analysis of its HRESIMS {*m/z* 503.2077 $[M - H]^-$}, ^{13}C NMR, and DEPT data. The ^1H NMR spectrum of **1** (Table 1) contains a typical ABX spin system [δ_H 6.67 (1H, d, J = 8.7 Hz, H-6), 6.60 (1H, dd, J = 8.7, 2.9 Hz, H-5), and 6.46 (1H, d, J = 2.9 Hz, H-3)] and an AA'BB' system [δ_H 6.80 (2H, d, J = 8.4 Hz, H-2″ and H-6″), δ_H 7.45 (2H, d, J = 8.4 Hz, H-3″ and H-5″)]. The ^{13}C NMR and DEPT spectra (Table 1) contain 30 resonances attributable to two methyls, six methylenes, twelve methines, and ten quaternary carbons (including two ester carbonyls and three oxygenated aromatic carbons). These signals suggest that **1** is a meroterpenoid analog [3]. Interpretation of 1D and 2D NMR data discloses that the structure of **1** resembles that of zizhine A [3] differing with an additional substituent at C-12′. The additional substituent contains one 1,4-disubstituted benzene substructure evidenced by the presence of the above AA'BB' system. In addition, one double bond [δ_H 7.60 (1H, d, J = 16.0 Hz, H-7″) and δ_H 6.33 (1H, d, J = 16.0 Hz, H-8″)] and a carbonyl group (δ_C 169.1, H-9″) is observed. The HMBC correlations (Fig. 2) of H-7″, H-8″/C-4″, C-9″ indicate the substituent is a 4-hydroxycinnamic acid, which is connected to C-12′ supported by the HMBC correlation of H-12′ (δ_H 4.54, s)/C-9″ via an ester linkage. The ROESY correlations of H-6′/H-8′, H-5′/H-14′, H-9′/H-13′ H-10′/H-12′, and the coupling constant between H-7″ and H-8″ (J = 16.0 Hz) suggest the geometry of the three double bonds are all *E*. Thus, the planar structure of **1** was elucidated. Compound **1** was found to be a racemate which was subjected to chiral HPLC to yield a pair of enantiomers (+)-**1**

* Corresponding author.
E-mail address: yxcheng@szu.edu.cn (Y.-X. Cheng).
[1] These authors contributed equally to this paper.

https://doi.org/10.1016/j.fitote.2019.03.016
Received 15 February 2019; Received in revised form 17 March 2019; Accepted 17 March 2019
Available online 20 March 2019
0367-326X/

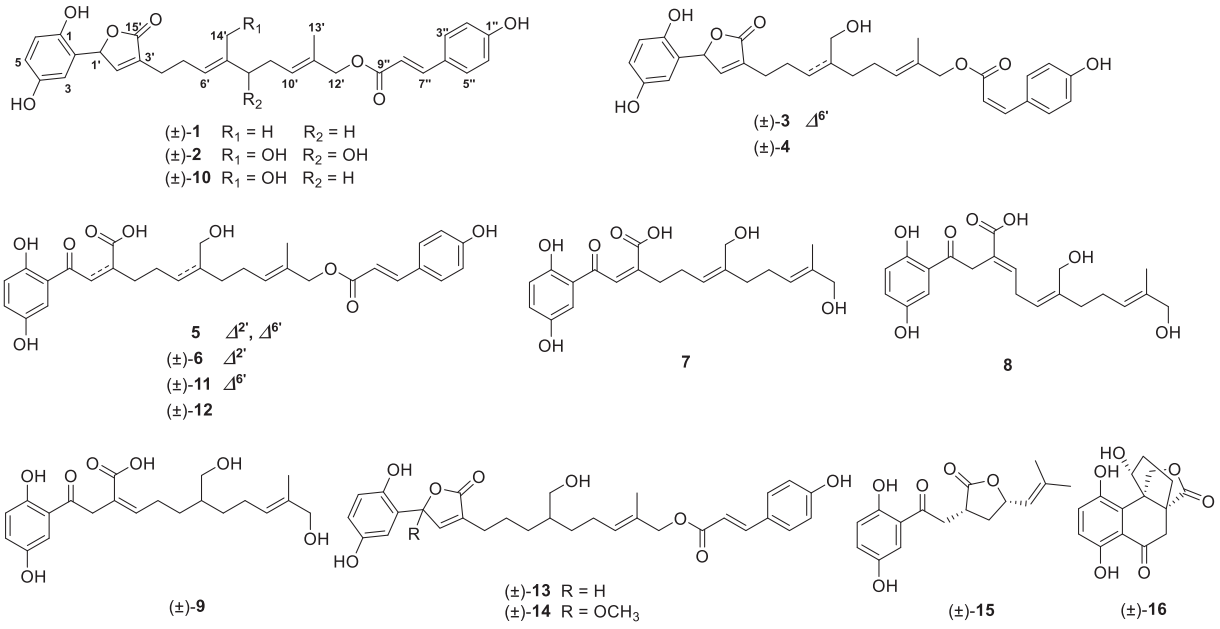

Fig. 1. The structures of compounds **1–16**.

Table 1
^{1}H and ^{13}C NMR data of compounds **1–5** (δ in ppm, J in Hz).

No.	1[a]		2[a]		3[b]		4[b]		5[c]	
	δ_H	δ_C	δ_H	δ_C	δ_H	δ_C	δ_H	δ_C	δ_H	δ_C
1		148.8		149.0		148.9		149.0		157.2
2		123.5		123.3		123.4		123.5		121.4
3	6.46 d (2.9)	113.2	6.46 d (2.9)	113.4	6.45 d (2.9)	113.3	6.47 d (2.9)	113.3	7.14 d (2.9)	115.8
4		151.5		151.4		151.5		151.5		150.8
5	6.60 dd (8.7, 2.9)	117.1	6.61 dd (8.6,2.9)	117.2	6.60 dd (8.7, 2.9)	117.2	6.61 dd (8.7, 2.9)	117.2	7.04 dd (8.9, 2.9)	126.7
6	6.67 d (8.7)	117.1	6.68 d (8.6)	117.3	6.67 d (8.7)	117.2	6.68 d (8.7)	117.3	6.83 d (8.9)	120.0
1′	6.21 br s	79.8	6.23 br s	79.9	6.23 br s	79.8	6.24 d (1.4)	79.9		198.6
2′	7.33 br s	151.3	7.37 br s	151.5	7.35 br s	151.5	7.35 d (1.4)	150.8	7.71 s	132.8
3′		132.9		132.8		132.8		133.7		146.1
4′	2.33 m	26.2	2.40 overlap	26.2	2.36 overlap	26.3	2.29 t (7.5)	26.4	2.66 t (7.6)	29.6
5′	2.28 m	26.9	2.40 overlap	26.4	2.36 overlap	26.5	1.60 m	26.0	2.32 m	28.2
6′	5.13 t (7.1)	124.5	5.58 t (7.3)	129.3	5.27 t (6.1)	127.7	1.43 m	31.5	5.27 t (7.7)	127.6
7′		137.3		142.5		140.6	1.48 m	40.9		140.4
8′	2.02 t (7.4)	40.1	4.16 overlap	75.3	2.15 overlap	35.3	1.35 m	31.6	2.08 m	35.1
9′	2.10 m	27.1	2.40 overlap	35.4	2.15 overlap	27.3	2.08 m	26.0	2.11 m	27.2
10′	5.45 t (7.2)	130.1	5.53 t (7.3)	126.6	5.43 t (6.6)	130.3	5.47 t (7.2)	130.8	5.44 t (6.9)	130.2
11′		131.6		133.1		131.5		131.4		131.6
12′	4.54 s	71.0	4.56 s	70.8	4.48 s	70.9	4.50 s	70.9	4.54 s	71.0
13′	1.67 s	14.1	1.69 s	14.4	1.61 s	14.2	1.63 s	14.2	1.66 s	14.1
14′a	1.58 s	16.2	4.16 overlap	58.1	4.06 d (12.3)	59.9	3.48 m	65.3	4.08 s	59.9
14′b					4.04 d (12.3)					
15′		176.8		176.7		176.7		176.8		170.1
1″		161.3		161.3		160.0		160.0		161.2
2″,6″	6.80 d (8.4)	116.8	6.80 d (8.4)	116.8	6.74 d (8.7)	115.9	6.74 d (8.4)	115.8	6.79 d (8.3)	116.8
3″,5″	7.45 d (8.4)	131.2	7.45 d (8.4)	131.2	7.59 d (8.7)	133.5	7.59 d (8.4)	133.5	7.44 d (8.3)	131.2
4″		127.1		127.1		127.7		127.7		127.1
7″	7.60 d (16.0)	146.6	7.61 d (16.0)	146.6	6.84 d (12.8)	144.8	6.84 d (12.7)	144.8	7.59 d (15.9)	146.5
8″	6.33 d (16.0)	115.2	6.33 d (16.0)	115.2	5.76 d (12.8)	116.8	5.77 d (12.7)	116.8	6.31 d (15.9)	115.2
9″		169.1		169.1		168.3		168.3		169.1

[a] 400 MHz for ^{1}H and 150 MHz for ^{13}C NMR in methanol-d_4.
[b] 800 MHz for ^{1}H and 200 MHz for ^{13}C NMR in methanol-d_4.
[c] 600 MHz for ^{1}H and 150 MHz for ^{13}C NMR in methanol-d_4.

{$[\alpha]_D^{20}$ +16.9 (*c* 0.07, MeOH); CD (MeOH) $\Delta\varepsilon_{209}$ + 20.58} and (−)-**1** {$[\alpha]_D^{20}$ −45.8 (*c* 0.08, MeOH); CD (MeOH) $\Delta\varepsilon_{211}$–20.45}, whose absolute configurations are assigned as 1′*R* and 1′*S*, respectively, by comparison of the specific rotation and experimental CD (circular dichroism) data with those of zizhine A. As a result, the structure of **1** was elucidated as shown (Fig. 1) and named zizhine G.

Analysis of the HREIMS, ^{13}C NMR, and DEPT spectra of zizhine H (**2**) shows it has a molecular formula of $C_{30}H_{32}O_9$ with two additional oxygen atoms than **1**, indicating fifteen degrees of unsaturation. The NMR data of **2** are also almost identical to those of **1**. Comparison of their NMR data (Table 1) reveals that the CH_2–8′ and CH_3–14′ in **1** are changed to CHOH-8′ and CH_2OH-14′ in **2**, which could be further

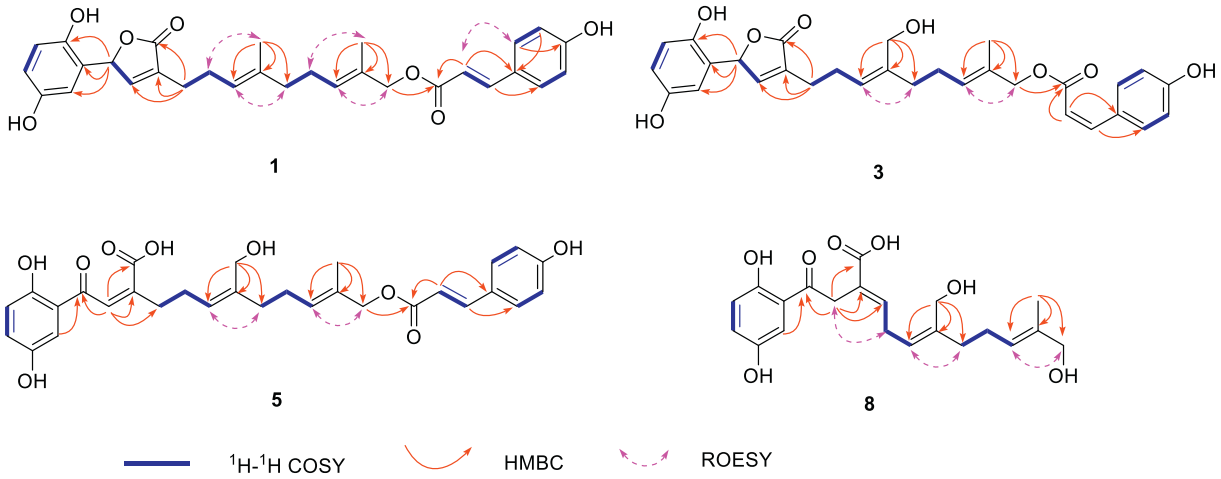

Fig. 2. ^{1}H−^{1}H COSY, key HMBC, and ROESY correlations of compounds **1**, **3**, **5**, and **8**.

certified by the ^{1}H−^{1}H COSY correlations of H-8′/H$_2$–9′/H-10′ and the HMBC correlations of H$_2$–14′, H-10′/C-8′ (δ_C 75.3), and H-6′, H-8′/C-14′ (δ_C 58.1). The *tran*-configurations of $\Delta^{6'(7')}$, $\Delta^{10'(11')}$ and $\Delta^{7''(8'')}$ were also deduced from the ROESY correlations of H-6′/H-8′, H-10′/H-12′, and $J_{7'',8''}$ value (16.0 Hz). Therefore, the planar structure of **2** was deduced. Compound **2** was also obtained as a racemate. Further chiral HPLC separation afforded (+)-**2** and (−)-**2**. Although we collected the optical rotation and CD data of two enantiomers, it is challenging to assign their absolute configurations using ECD calculations due to the presence of many conformers resulting from the free rotation of the side chain. Besides, theoretically it is possible to use Mosher's methods to assign the absolute configuration at C-8′, however, the limit of the amount prohibited our further efforts. Collectively, the structure of (±)-**2** was determined as shown in Fig. 1.

The HRESIMS and NMR data of zizhine I (**3**) indicate that it has the same molecular formula as that of ganosinensols A and B [10]. Careful comparison of the NMR data between **3** and **10** found that they differ from the geometry at $\Delta^{7''(8'')}$ double bond, which is a *trans*-orientation in **10** but a *cis*-orientation in **3** evidenced by the coupling constant between H-7″ and H-8″ (J = 12.8 Hz). Compound **3** is racemic based on chiral HPLC analysis and its negligible specific rotation value {$[\alpha]_D^{24}$ –6.3 (*c* 0.08, MeOH)}. Further chiral separation was not conducted due to the limited amount of (±)-**3**. However, it is easy to assign (+)-**3** as 1′*R* and (−)-**3** as 1′*S*, respectively, according to the absolute configuration of **1**.

Zizhine *J* (**4**) has a molecular formula of $C_{30}H_{34}O_8$ established from an ion peak at *m/z* 521.2179 [M–H]$^-$ in the HRESIMS in combination of the NMR data, indicating fourteen degrees of unsaturation. Detailed NMR data interpretation of **4** and **3** (Table 1) reveals that they are almost identical excepting for a less degree of unsaturation in **4** attributed to the reduction of $\Delta^{6'(7')}$. The ^{1}H−^{1}H COSY correlations of H$_2$–6′/H-7′/H$_2$–8′/H$_2$–9′ and H-7′/H$_2$–14′ give the further certification. Although compound **4** is also optically inactive, further separation by chiral HPLC was not successful due to the poor resolution. So far, the absolute configurations at C-1′ and C-7′ in **4** remain unknown.

Zizhine K (**5**) possesses a molecular formula of $C_{30}H_{32}O_9$ established from an ion peak at *m/z* 535.1963 [M − H]$^-$ in the HRESIMS, in combination of the NMR data, indicating fifteen degrees of unsaturation. The ^{1}H NMR spectrum of **5** indicates a typical ABX system (δ_H 7.14, d, J = 2.9 Hz, H-3; δ_H 7.04, dd, J = 8.9, 2.9 Hz, H-5; δ_H 6.83, d, J = 8.9 Hz, H-6). The ^{13}C NMR and DEPT spectra display 30 carbons ascribed to one methyl, six methylenes, twelve methines and eleven quaternary carbons (including one ketone carbonyl, two ester carbonyls, three olefinic, and five aromatic with three oxygenated). The NMR data of the aromatic nucleus in **5** are identical to those of **10**, and their side chains are also similar to some extent from C-2′ to C-14′. The HMBC correlations of H-3/C-1′ (δ_C 198.6), H-2′ (δ_H 7.71)/C-1′, C-3′ (δ_C 146.1), C-4′ (δ_C 29.6), and C-15′ (δ_C 170.1) demonstrate the lactone ring in **5** is broken and C-1′ is further oxygenated to a ketone. Thus, the planar structure of **5** was deduced as shown (Fig. 1). In the ROESY spectrum, ROESY correlations of H-6′/H-8′ and H-10′/H-12′ are observed, in consideration of $J_{7'',8''}$ value (15.9 Hz), suggesting the configurations of the double bonds $\Delta^{6'(7')}$, $\Delta^{10'(11')}$, and $\Delta^{7''(8'')}$ were *cis*, *trans*, and *trans*-orientation, respectively. Thus, the structure of zizhine K was assigned.

Zizhine L (**6**) has the molecular formula of $C_{30}H_{34}O_9$ (fourteen degrees of unsaturation) based on its HRESIMS, ^{13}C NMR, and DEPT data. A detailed comparison of the ^{1}H and ^{13}C NMR data (Table 2) between **6** and **5** discloses that **6** is a reduced product of **5** with the loss of the $\Delta^{6'(7')}$ double bond. The ^{1}H−^{1}H COSY correlations of H$_2$–6′/H-7′/H$_2$–8′/H$_2$–9′ and H-7′/H$_2$–14′ give the further certification. Compound **6** is also a racemate by chiral HPLC analysis. Further separation of racemic **6** was not continued due to poor peak resolution even at optimized chromatographic conditions. The only one chiral center present in **6** indicates that the absolute configuration of the two enantiomers at C-7′ is 7′*R* or 7′*S*.

Zizhine M (**7**) has a molecular formula $C_{21}H_{26}O_7$ (9 degrees of unsaturation) derived from analysis of its HRESIMS, ^{13}C NMR and DEPT data. Interpretation of 1D and 2D NMR data discloses that **7** and **5** are analogs. The difference is that the substituent group of 4-hydroxycinnamic acid in **5** is absent in **7**. The key ^{1}H−^{1}H COSY and HMBC correlations also support this alteration. The ROESY correlations of H-2′/H-4′, H-5′/H-14′, and H-10′/H-12′ indicate the *Z*-form of $\Delta^{2'(3')}$ and $\Delta^{6'(7')}$ double bonds, and the *E*-form of $\Delta^{10'(11')}$ double bond. In this way, the structure **7** was finally identified.

The HRESIMS and NMR data of zizhine N (**8**) indicate that it has the same molecular formula as that of **7**. Careful comparison of the NMR data of **8** with those of **7** reveals that they bear the same planar structure. The obvious difference is that the $\Delta^{2'(3')}$ double bond in **7** is migrated to $\Delta^{3'(4')}$ in **8**, supported by the ^{1}H−^{1}H COSY correlations of H-4′/H-5′/H-6′. In addition, the ROESY correlations of H$_2$–2′/H$_2$–5′, H-6′/H$_2$–8′, and H-10′/H$_2$–12′ indicate the *E*-orientation *of* $\Delta^{3'(4')}$ and $\Delta^{10'(11')}$ double bonds, and *Z*-orientation of the $\Delta^{6'(7')}$ double bond. Thus, the structure of zizhine N was assigned.

Zizhine O (**9**) has the molecular formula $C_{21}H_{28}O_7$ derived from analysis of its HRESIMS and 1D NMR data, with two more protons than **8**. Likewise, its NMR data (Table 2) are almost identical to those of **8** differing from the absence of $\Delta^{6'(7')}$ double bond and the *Z*-orientation of $\Delta^{3'(4')}$ double bond, supported by the ^{1}H−^{1}H COSY correlations of H$_2$–6′, H$_2$–14′/H-7′/H$_2$–8′/H$_2$–9′ and the ROESY correlation of H$_2$–2′/H-4′. Compound **9** was isolated as a racemate judged by its chiral HPLC analysis. Thus, the absolute configuration of the sole chiral center in the

Table 2
^{1}H (600 MHz) and ^{13}C (150 MHz) NMR data of compounds **6–9** (δ in ppm, J in Hz).

No.	6		7		8		9	
	δ_H	δ_C	δ_H	δ_C	δ_H	δ_C	δ_H	δ_C
1		157.2		157.2		156.5		156.4
2		121.4		121.4		120.6		121.0
3	7.15 d (2.9)	115.8	7.16 d (2.9)	115.8	7.36 d (2.9)	115.7	7.39 d (2.9)	116.0
4		150.8		150.8		150.7		150.6
5	7.04 dd (8.9, 2.9)	126.7	7.04 dd (8.9, 2.9)	126.6	7.01 dd (8.9, 2.9)	125.8	6.96 dd (8.9, 2.9)	125.4
6	6.84 d (8.9)	119.9	6.84 d (8.9)	119.9	6.80 d (8.9)	119.6	6.76 d (8.9)	119.5
1′		198.8		198.7		204.5		205.9
2′	7.66 s	132.2	7.69 s	132.1	4.10 s	37.3	4.00 s[a]	38.5[a]
3′		147.2		147.2		128.4		133.2
4′	2.59 m	29.7	2.68 t (7.5)	29.6	6.97 t (7.8)	144.4	6.75 t (7.6)	141.2
5′	1.55 m	27.6	2.32 m	28.2	3.00 t (7.5)	28.4	2.16 m	27.3
6′a	1.40 m	31.7	5.27 t (7.7)	127.4	5.31 t (7.4)	124.5	1.52 m	31.2
6′b								1.32 m
7′	1.46 m	40.7		140.7		141.6	1.51 m	40.9
8′	1.31 m	31.3	2.05 m	35.4	2.17 overlap	35.7	1.41 m	31.8
9′	2.07 m	25.9	2.07 m	27.3	2.17 overlap	27.3	2.05 m	25.9
10′	5.49 t (7.3)	130.8	5.35 t (6.6)	126.7	5.40 t (7.1)	126.3	5.37 t (7.3)	127.0
11′		131.5		135.9		136.2		135.9
12′	4.55 s	71.2	3.89 s	69.0	3.91 s	68.9	3.89 s	69.0
13′	1.69 s	14.1	1.61 s	13.8	1.64 s	13.8	1.62 s	13.7
14′	3.45 m	65.4	4.06 s	59.9	4.10 s	60.0	3.47 d (4.8)	65.2
15′		170.4		170.7		171.6		176.0
1″		161.2						
2″,6″	6.79 d (8.3)	116.8						
3″,5″	7.45 d (8.3)	131.2						
4″		127.2						
7″	7.60 d (15.9)	146.5						
8″	6.32 d (15.9)	115.2						
9″		169.2						

[a] Assigned by HSQC and HMBC data.

two enantiomers at C-7′ was assigned to be 7′*R* or 7′*S*, respectively.

In addition to the new substances described above, the seven known meroterpenoids were respectively identified as ganosinensols A ((−)-**10**) and B ((+)-**10**) [10], ganoduriporols A and B (**11** and **12**) [11], zizhines P (**13**) and Q (**14**) [12], chizhine B (**15**) [13], and lingzhiol (**16**) [14] by comparing their NMR data with the literature data.

The AchE inhibitory activities of all the compounds except for (+)-**10**, **15**, and **16** were evaluated, The results (Table 3) show that (+)-**1**, (−)-**1**, (−)-**10**, (+)-**13**, (−)-**13**, (+)-**14**, and (−)-**14** exhibit inhibitory activities toward AchE with the inhibition rates of 88.77%, 87.68%, 82.18%, 89.24%, 87.73%, 83.43%, and 83.71%, respectively, at the concentration of 50 μM (tacrine was used as a positive control with an IC_{50} value of 0.20 ± 0.02 μM. Whereas, compounds **7–9** are almost inactive in this assay. Analysis of these biological results discloses that the presence of the hydroxycinnamoyl group is very important for keeping activity. The inhibition potency aganist AchE appears not to be affected by their enantiomeric purity in the case of compounds **1**, **2**, **13**, and **14**. The inhibition of compounds **1** and **10** is stronger than that of **2**, indicating that 8'-OH is not favourable for keeping the activity. In addition, the biological difference between compounds **5**, **6**, **11**, and **12** and compounds **1**, **10**, **13**, and **14** suggests the importance of the presence of a five-membered lactone.

Table 3
The AchE inhibition activity of the selected compounds at 50 μM.

Compd.	Inhibition ratio (%)	Compd.	Inhibition ratio (%)
(+)-**1**	88.77 ± 0.44	(±)-**9**	12.67 ± 4.09
(−)-**1**	87.68 ± 0.17	(−)-**10**	82.18 ± 0.20
(+)-**2**	48.32 ± 0.56	(±)-**11**	58.66 ± 0.95
(−)-**2**	50.33 ± 0.44	(±)-**12**	67.69 ± 0.30
(±)-**3**	66.75 ± 0.78	(+)-**13**	89.24 ± 0.26
(±)-**4**	73.21 ± 1.29	(−)-**13**	87.73 ± 0.58
5	63.78 ± 0.86	(+)-**14**	83.43 ± 0.05
(±)-**6**	63.30 ± 0.95	(−)-**14**	83.71 ± 0.41
7	13.19 ± 5.09	**Tacrine**[a]	60.68 ± 2.85
8	24.78 ± 1.57		

[a] The concentration used is 0.33 μM.

3. Experimental section

3.1. General experimental procedures

Optical rotations were recorded on a Jasco P-1020 digital polarimeter. UV spectra were measured on a Shimadzu UV2401PC spectrometer. CD spectra were measured on an Applied Photophysics Chirascan instrument. NMR spectra were measured on a Bruker AV 400, 600 or 800 MHz spectrometer, with TMS as an internal standard. ESIMS and HRESIMS were measured on an Agilent 1290 UPLC/6540 Q-TOF instrument. RP-18 (40–63 μm, Daiso Co., Japan), MCI gel CHP 20P (75–150 μm, Tokyo, Japan), silica gel GF254 (80–100 mesh, Qingdao Marine Chemical Inc., P.R. China), and Sephadex LH-20 (Amersham Biosciences, Sweden) were used for column chromatography. Semi-preparative HPLC was carried out using an Agilent 1200 liquid chromatograph and a LC-3000 high liquid chromatograph (P.R. China), the columns used were YMC-Pack ODS-A (250 mm × 10 mm, i.d., 5 μm) and Daicel Chiralpak IC (250 mm × 10 mm, i.d., 5 μm), flow rate: 2.5 mL/min.

3.2. Fungal material

The fruiting bodies of *G. sinensis* were purchased from Tongkang Pharmaceutical Co. Ltd. in Guangzhou Province, P.R. China, in September 2013. The material was identified by Prof. Zhu-Liang Yang at Kunming Institute of Botany, Chinese Academy of Sciences, and a voucher specimen (CHYX0591) has been deposited at School of

Pharmaceutical Sciences, Shenzhen University since November 2017.

3.3. Extraction and isolation

Dried and powdered *G. sinensis* (40.0 kg) was extracted with aqueous EtOH under reflux (70%, 3 × 130 L × 2 h) to give a crude extract, which was suspended in H_2O followed by extraction with EtOAc to afford an EtOAc extract (0.72 kg). The EtOAc extract was divided into eight parts (Fr.1–Fr.8) by using a MCI gel CHP 20P column chromatography eluted with aqueous MeOH (20%–100%).

Fr.3 (18.0 g) was subsequently separated by RP-18 eluted with aqueous MeOH (20%–60%) to get six portions (Fr.3.1 − Fr.3.6). Fr.3.3 (1.5 g) was filtered by Sephadex LH-20 (MeOH) to give Fr.3.3.1 − Fr.3.3.3. Fr.3.3.2 (0.2 g) was firstly subjected to a prep-TLC ($CHCl_3$/MeOH, 10:1) followed by Sephadex LH-20 (MeOH) to obtain **16** (1.7 mg). Fr.3.6 (1.2 g) was firstly filtered by Sephadex LH-20 (MeOH) to give Fr.3.6.1 and Fr.3.6.2. Of which, Fr.3.6.1 was then subjected to a prep-TLC ($CHCl_3$/MeOH, 8:1), and further purified by Sephadex LH-20 (MeOH) to obtain **8** (9.2 mg) and **9** (6.7 mg). Fr.4 (10.7 g) was separated by RP-18 eluted with aqueous MeOH (30%–60%) to get five portions (Fr.4.1 − Fr.4.5). Fr.4.2 (2.0 g) was separated by Sephadex LH-20 (MeOH) followed by semi-preparative HPLC (MeOH/H_2O, 65%) to yield **7** (17.9 mg). Fr.5 (29.0 g) was separated by MCI gel CHP 20P eluted with aqueous MeOH (30%–70%) to provide four portions (Fr.5.1 − Fr.5.4). Of them, Fr.5.4 (8.8 g) was subjected to a RP-18 column eluted with aqueous MeOH (45%–80%) to give Fr.5.4.1–Fr.5.4.5. Fr.5.4.4 (2.3 g) was further purified by Sephadex LH-20 (MeOH) followed by semi-preparative HPLC (MeOH/H_2O, 62%) to yield **2** (3.0 mg). Fr.6 (32.0 g) was separated by MCI gel CHP 20P column eluted with aqueous MeOH (40%–60%) to provide seven portions (Fr.6.1 − Fr.6.7). Fr.6.5 (2.0 g) was subjected to gel filtration over Sephadex LH-20 (MeOH) to obtain Fr.6.5.1 − Fr.6.5.5. Of which, Fr.6.5.4 (0.3 g) was firstly separated by prep-TLC ($CHCl_3$/MeOH, 7:1) and then purified by semi-preparative HPLC (MeOH/H_2O, 66%) to give compounds **10** (4.0 mg), **3** (0.8 mg), **13** (6.5 mg), **14** (6.5 mg), and **4** (0.8 mg). Fr.6.6 (13.0 g) was subjected to a RP-18 column eluted with aqueous MeOH (55%–65%) to give Fr.6.6.1 and Fr.6.6.2. Fr.6.6.1 (8.0 g) was fractionated by Sephadex LH-20 (MeOH) followed by semi-preparative HPLC (MeOH/H_2O, 68%) to give compound **15** (3.3 mg). Fr.6.7 (9.3 g) was separated by RP-18 eluted with aqueous MeOH (40%–80%) to afford Fr.6.7.1–Fr.6.7.3. Fr.6.7.2 (3.0 g) was firstly submitted to a silica gel column eluted with petroleum ether/acetone system (from 15:1 to 1:1), and then fractionated by Sephadex LH-20 (MeOH) and semi-preparative HPLC (ACN/H_2O, 45%) to afford compound **11** (9.6 mg). Fr.6.7.3 (3.2 g) was firstly subjected to Sephadex LH-20 (MeOH), and then prep-TLC ($CHCl_3$/MeOH, 5:1) and semi-preparative HPLC (MeOH /H_2O, 75%) to afford compounds **5** (12.0 mg), **6** (8.0 mg), and **12** (4.5 mg). Fr.7 (23.0 g) was submitted to a RP-18 column eluted with aqueous MeOH (50%–100%) to afford Fr.7.1–Fr.7.4. Of which, Fr.7.2 (2.7 g) was firstly purified by Sephadex LH-20 (MeOH) and then followed by semi-preparative HPLC (MeOH/H_2O, 70%) to produce compound **1** (3.2 mg).

Furthermore, racemic compounds **1**, **2**, **10**, **13**, and **14** were separated by chiral HPLC (flow rate: 2.5 mL/min) to yield their respective enantiomers, (+)-**1** (1.3 mg) and (−)-**1** (1.2 mg) (*n*-hexane/ethanol, 68:32); (+)-**2** (1.1 mg) and (−)-**2** (1.0 mg) (*n*-hexane/ethanol, 70:30); (+)-**10** (1.6 mg) and (−)-**10** (1.4 mg) (*n*-hexane/ethanol, 66:34); (+)-**13** (2.8 mg) and (−)-**13** (2.5 mg) (*n*-hexane/ethanol, 68:32); (+)-**14** (2.7 mg) and (−)-**14** (2.8 mg) (*n*-hexane/ethanol, 66:34).

Zizhine G (**1**): yellowish gum; UV (MeOH) λ_{max} (logε) 381 (3.05), 310 (4.34), 203 (4.59) nm; {$[\alpha]_D^{20}$ +16.9 (*c* 0.07, MeOH); CD (MeOH) $\Delta\varepsilon_{209}$ + 20.58; (+)-**1**}; {$[\alpha]_D^{20}$ −45.8 (*c* 0.08, MeOH); CD (MeOH) $\Delta\varepsilon_{211}$–20.45; (−)-**1**}; ESIMS *m/z* 503 $[M–H]^-$, HRESIMS (negative) *m/z* 503.2077 $[M - H]^-$ (calcd for $C_{30}H_{31}O_7$, 503.2075); ^1H and ^{13}C NMR data, see Table 1.

Zizhine H (**2**): yellowish gum; UV (MeOH) λ_{max} (logε) 310 (4.25), 221 (4.31), 202 (4.55) nm; {$[\alpha]_D^{18}$ +8.1 (*c* 0.08, MeOH); CD (MeOH) $\Delta\varepsilon_{211}$ + 5.61; (+)-**2**}; {$[\alpha]_D^{19}$ −11.8 (*c* 0.06, MeOH); CD (MeOH) $\Delta\varepsilon_{209}$–8.60; (−)-**2**}; ESIMS *m/z* 535 $[M–H]^-$, HRESIMS (negative) *m/z* 535.1975 $[M - H]^-$ (calcd for $C_{30}H_{31}O_9$, 535.1974); ^1H and ^{13}C NMR data, see Table 1.

Zizhine I (**3**): yellow gum; $[\alpha]_D^{24}$ –6.3 (*c* 0.08, MeOH); UV (MeOH) λ_{max} (log ε) 310 (4.06), 204 (4.29) nm; ESIMS *m/z* 519 $[M–H]^-$, HRESIMS *m/z* 519.2022 $[M–H]^-$ (calcd for $C_{30}H_{31}O_8$, 519.2024).^1H and ^{13}C NMR data, see Table 1.

Zizhine *J* (**4**): yellow gum; $[\alpha]_D^{24}$ –8.8 (*c* 0.08, MeOH); UV (MeOH) λ_{max} (logε) 309 (4.14), 203 (4.29) nm; ESIMS *m/z* 521 $[M–H]^-$, HRESIMS *m/z* 521.2179 $[M–H]^-$ (calcd for $C_{30}H_{33}O_8$, 521.2181). ^1H and ^{13}C NMR data, see Table 1.

Zizhine K (**5**): yellowish gum; UV (MeOH) λ_{max} (logε) 294 (4.40), 226 (4.38), 202 (4.54) nm; ESIMS *m/z* 535 $[M–H]^-$, HRESIMS *m/z* 535.1963 $[M - H]^-$ (calcd for $C_{30}H_{31}O_9$, 535.1968); ^1H and ^{13}C NMR data, see Table 1.

Zizhine L (**6**): yellowish gum; UV (MeOH) λ_{max} (logε) 293 (4.34), 226 (4.31), 202 (4.43) nm; ESIMS *m/z* 537 $[M–H]^-$, HRESIMS *m/z* 537.2131 $[M - H]^-$ (calcd for $C_{30}H_{33}O_9$, 537.2125); ^1H and ^{13}C NMR data, see Table 2.

Zizhine M (**7**): yellow gum; UV (MeOH) λ_{max} (logε) 383 (3.50), 267 (3.96), 221 (4.07), 202 (4.30) nm; ESIMS *m/z* 389 $[M–H]^-$, HRESIMS *m/z* 389.1607 $[M–H]^-$ (calcd for $C_{21}H_{25}O_7$, 389.1606); ^1H and ^{13}C NMR data, see Table 2.

Zizhine N (**8**): yellow gum; UV (MeOH) λ_{max} (logε) 363 (3.56), 250 (4.02), 219 (4.35), 203 (4.40) nm; ESIMS *m/z* 389 $[M–H]^-$, HRESIMS *m/z* 389.1605 $[M–H]^-$ (calcd for $C_{21}H_{25}O_7$, 389.1606); ^1H and ^{13}C NMR data, see Table 2.

Zizhine O (**9**): yellow gum; UV (MeOH) λ_{max} (logε) 352 (3.25), 250 (3.69), 206 (4.09) nm; ESIMS *m/z* 391 $[M–H]^-$, HRESIMS *m/z* 391.1764 $[M–H]^-$ (calcd for $C_{21}H_{27}O_7$, 391.1762); ^1H and ^{13}C NMR data, see Table 2.

3.4. AchE inhibition

Inhibition of AchE activity was assayed using a microplate as previously described [15,16]. Briefly, 110 μL of PBS buffer (pH 8), 10 μL positive controls or compounds with different concentrations (dissolved in DMSO), 40 μL of 0.1 U/mL AchE (diluted with PBS buffer, Sigma) were added to 96-well plate and then incubate at 37 °C for 20 min in ELIASA (Multiskan FC, Thermo). Thereafter, 20 μL of 6.25 mM 5,5′-dithiobis (2-nitrobenzoic acid) (Sigma) and 20 μL of 6.25 mM acetylthiocholine iodide (Sigma) were added. Then, the absorbance was measured at 405 nm every 30 s for 20 times. Tacrine was used as the positive control. The assay was done in triplicate and the results are expressed as mean ± SD.

Conflict of interest

We declare no conflict of interest for this study.

Acknowledgments

This work was supported by National Key Research and Development Program of China (2017YFA0503900) and National Science Fund for Distinguished Young Scholars (81525026).

Appendix A. Supplementary data

Supplementary data to this article can be found online at https://doi.org/10.1016/j.fitote.2019.03.016.

References

[1] Y.Q. Zhou, X.T. Yang, Q.Y. Yang, Recent advances on triterpenes from Ganoderma

mushroom, Food Rev. Int. 22 (2006) 259–273.
[2] S.C. Jong, J.M. Birmingham, Medicinal benefits of the mushroom *Ganoderma*, Adv. Appl. Microbiol. 37 (1992) 101–134.
[3] W.W. Cao, Q. Luo, Y.X. Cheng, S.M. Wang, Meroterpenoid enantiomers from *Ganoderma sinensis*, Fitoterapia 110 (2016) 110–115.
[4] W.G. Zhang, X. Liu, Isolation, purification and structure analysis of polysaccharide I from solid fermented mycelia of *Ganoderma sinensis* 9519, Chem. Bioeng. 23 (2006) 32–37.
[5] J.P. Zhang, L. Zheng, J.H. Wang, K.E. Magnusson, X. Liu, Lipid extract from completely sporoderm-broken germinating *Ganoderma sinensis* spores elicits potent antitumor immune responses in human macrophages, Phytother. Res. 23 (2010) 844–850.
[6] N. Sato, C.M. Ma, K. Komatsu, M. Hattori, Triterpene-farnesyl hydroquinone conjugates from *Ganoderma sinense*, J. Nat. Prod. 72 (2009) 958–961.
[7] Q. Luo, L. Tian, Y.M. Yan, L. Di, Y.X. Cheng, (±)-Sinensilactam A, a pair of rare hybrid metabolites with smad3 phosphorylation inhibition from *Ganoderma sinensis*, Org. Lett. 17 (2015) 1565–1568.
[8] M. Dou, L. Di, L.L. Zhou, Y.M. Yan, X.L. Wang, F.J. Zhou, Z.L. Yang, R.T. Li, F.F. Hou, Y.X. Cheng, Cochlearols A and B, polycyclic meroterpenoids from the fungus *Ganoderma cochlear* that have renoprotective activities, Org. Lett. 16 (2014) 6064–6067.
[9] Q. Luo, L. Di, W.F. Dai, Q. Lu, Y.M. Yan, Z.L. Yang, R.T. Li, Y.X. Cheng, Applanatumin A, a new dimeric meroterpenoid from *Ganoderma applanatum* that displays potent antifibrotic activity, Org. Lett. 17 (2015) 1110–1113.
[10] M. Wang, F. Wang, F. Xu, L.Q. Ding, Q. Zhang, H.X. Li, F. Zhao, L.Q. Wang, L.H. Zhu, L.X. Chen, F. Qiu, Two pairs of farnesyl phenolic enantiomers as natural nitric oxide inhibitors from *Ganoderma sinense*, Bioorg. Med. Chem. Lett. 26 (2016) 3342–3345.
[11] J.Q. Liu, C.L. Lian, T.Y. Hu, C.F. Wang, Y. Xu, L. Xiao, Z.Q. Liu, S.Q. Qiu, B.H. Cheng, Two new farnesyl phenolic compounds with anti-inflammatory activities from *Ganoderma duripora*, Food Chem. 263 (2018) 155–162.
[12] L.X. Chen, H. Li, Y. Gao, J. Guo, L.H. Zhu, Farnesyl phenol compound and preparation method and application, CN108689970 A, 20181023.
[13] Q. Luo, X.L. Wang, L. Di, Y.M. Yan, Q. Lu, X.H. Yang, D.B. Hu, Y.X. Cheng, Isolation and identification of renoprotective substances from the mushroom *Ganoderma lucidum*, Tetrahedron 71 (2015) 840–845.
[14] Y.M. Yan, J. Ai, L.L. Zhou, A.C.K. Chung, R. Li, J. Nie, P. Fang, X.L. Wang, J. Luo, Q. Hu, F.F. Hou, Y.X. Cheng, Lingzhiols, unprecedented rotary door-shaped meroterpenoids as potent and selective inhibitors of p-Smad3 from *Ganoderma lucidum*, Org. Lett. 15 (2013) 5488–5491.
[15] G.L. Ellman, D.K. Lourtney, V. Andres, G. Gmelin, A new and rapid colorimetric determination of acetylcholinesterase activity, Biochem. Pharmacol. 7 (1961) 88–95.
[16] K. Ingkaninan, P. Temkitthawon, K. Chuenchom, T. Yuyaem, W. Thongnoi, Screening for acetylcholinesterase inhibitory activity in plants used in Thai traditional rejuvenating and neurotonic remedies, J. Ethnopharmacol. 89 (2003) 261–264.